

锌基合金钎焊界面区的反应机制及组织结构

刘秀忠^{1,2}, 杨 敏^{1,2}, 刘性红³

(1. 山东大学 材料液态结构及其遗传性教育部重点实验室, 济南 250061;
2. 山东大学 材料科学与工程学院, 济南 250061;
3. 象山同家铸造模具厂, 浙江 象山 315700)



刘秀忠

摘 要: 采用 XRD, EPMA, TEM 和 SEM 等分析测试手段, 对用自行研制的钎料和钎剂钎焊的锌基合金钎焊接头界面区微区成分、组织精细结构及物相等进行了分析. 结果表明, 钎焊接头界面区主要有扩散区和溶解区组成, 扩散区中含有较多锡基固溶体 (1.44% Zn), 溶解区内含有较多的锌基固溶体, 整个界面区主要由锡、锡、锌、铝基固溶体及一些氧化物 SnO, SnO₂, CdO 和金属化合物 MgZn, Mg₂Sn, Al₄Cu₉, Mg₂Cu₆Al₅ 等组成, 未发现对钎焊接头性能有严重不利影响的连续状金属化合物层.

关键词: 锌基合金; 界面区; 反应机制; 组织结构

中图分类号: TG146 **文献标识码:** A **文章编号:** 0253-360X(2009)11-0089-04

0 序 言

锌基合金是近年来研制和快速发展的一种新型有色金属材料, 具有较高的强度、硬度、耐磨性及较好的流动性、可重复利用和生产成本低等优点, 目前已在机械、轻工、仪表、电机、塑料等行业得到越来越多的应用. 但其连接及修复技术和工艺是影响其快速发展的主要障碍. 目前对锌基合金的连接及其连接性能的研究仍处于探索研究阶段, 有很多技术和理论问题有待进一步探讨和解决.

锌基合金中的主要合金元素是 Al, Cu, Mg 及少量的稀土、Ti 等, 都是较活泼的金属元素, 锌的沸点低(仅为 906 ℃), 熔化焊的高温加热, 很容易产生锌及其合金元素的蒸发、氧化和烧损, 使焊缝及熔合区的成分、组织及性能发生变化, 获得的钎焊接头无法满足使用性能要求. 而钎焊连接时母材不熔化, 其加热温度低, 可减少锌的蒸发、氧化和烧损, 同时还可降低焊接应力, 防止过热对母材组织和性能的影响, 因此钎焊是解决高强度锌基合金连接和修复的最好方法之一^[1,2].

用自行研制的一种新型高强度软钎料, 配合自行研制的钎剂, 用炉中钎焊的方法, 对高强度锌基合金进行了钎焊; 用电子探针对钎焊接头界面区的组织形态和成分进行了分析测试; 用光学和电子显微

镜对钎焊接头界面区的微观组织结构、特征等进行了分析. 结果发现, 钎焊界面区由于合金元素的相互扩散、溶解等, 出现了局部的交互结晶, 这有利于提高钎缝和母材的结合强度. 经检索, 目前国内外还没有对高强度锌基合金的钎焊界面区组织及形态的研究报道, 因此作者对高强度锌基合金的钎焊性理论研究具有十分重要的意义.

1 试验方法

母材为一种新型高强度锌基合金, 用金属型铸成 120 mm×80 mm×8 mm 的试板, 其化学成分和力学性能见表 1. 钎料为自行研制的软钎料, 主要成分为锡、锡和锌, 其主要性能见表 2. 钎剂为自行研制的钎剂, 主要成分为 ZnCl₂, NH₄Cl, KF 等. 钎焊设备为空气电阻加热炉.

表 1 母材的化学成分和力学性能

Table 1 Chemical composition and mechanical properties of base material

化学成分(质量分数 %)						力学性能	
Al	Cu	Mn	Mg, Ti, Tm	Zn		抗拉强度 <i>R_m</i> /MPa	断后伸长率 <i>A</i> (%)
9.0~12.0	3.0~5.0	0.2~0.3	≤0.2	余量		≥300	>3

先用丙酮对试件待焊处进行清洗, 然后用细砂

表 2 钎料的主要性能

Table 2 Properties of soldering material

抗拉强度 R_m /MPa	断后伸长率 A_e /%	润湿角 θ / $^{\circ}$	熔点 T / $^{\circ}$ C
114	5.3	≤ 18	180~250

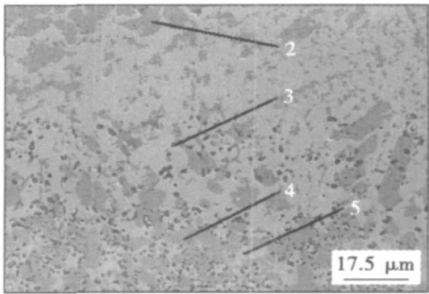
纸打磨以露出金属光泽. 在钎焊处放置适量的钎料和钎剂, 放入电阻炉中, 调整好钎焊工艺参数 (加热温度为 $320\text{ }^{\circ}\text{C}\pm 10\text{ }^{\circ}\text{C}$, 保温时间为 $15\text{ min}\pm 2\text{ min}$). 钎焊完成后将试板从炉中取出, 待其冷却到 $50\text{ }^{\circ}\text{C}$ 以下时, 用清水对钎焊处进行清洗, 然后进行外观质量检查, 最后根据不同的要求截取并制备成不同的试样. 用显微镜、扫描电镜等对钎焊接头界面区组织及其形态、微观组织特征等进行研究分析; 用电子探针分析仪对界面区成分进行分析测试, 并用 X 射线衍射仪分析界面区的相组成等.

2 试验结果及分析

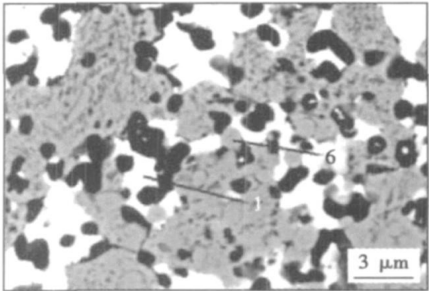
2.1 钎焊接头界面区的微区成分及组织

钎焊接头界面区的微观组织成分分析结果见表 3 和图 1. 从图 1 中可以看出, 界面区主要由两部分组成, 一部分为靠近钎缝的扩散区, 另一部分为靠近母材的溶解区. 该区域的组织和成分有很大的不均匀性. 白色基体组织 (测试点 1) 是含有 1.44% Zn 的锡固溶体; 靠近钎缝的大块状深色组织 (测试点 2) 中锌的含量高达 97% , 说明该组织是母材向钎料中溶解所形成的; 靠近母材界面区中的黑色点状组织 (测试点 3) 中含有较多的锡和铝, 并含有少量的锌和铜; 靠近母材界面区中的深色块状组织 (测试点 4) 的形态和测试点 2 的组织形态相似, 但成分中没有了锡, 只有 Zn, Al, Cu 三种元素, 且铜含量较高, 该组织中可能存在富铜的化合物; 靠近母材的浅色基体组织 (测试点 5) 和钎缝中浅色组织 (测试点 1) 的成分相近, 也是含有锌的锡固溶体, 其中锌的含量为

1.32% ; 靠近母材的界面区中点状组织的中含有较多的锌 (78.13%) 和铜 (12.63%), 同时还含有 5.74% 的锡和 3.51% 的铝, 说明该组织中应既有固溶体又有金属间化合物.



(a) 靠近钎缝的界面区组织形貌



(b) 靠近母材的界面区组织形貌

图 1 钎焊接头微观组织形貌

Fig. 1 Characteristic of microstructure in soldered joint

2.2 钎焊接头界面区微观组织及结构

钎焊界面区 X 射线衍射分析结果见图 2. 从图 2 中可以看出, 界面区的物相组成较复杂, 因为该区域在钎焊过程中, 母材和钎料的相互溶解和扩散较充分, 钎料及母材的大部分组分都能通过溶解和扩散到达该区, 形成组织和成分十分复杂的过渡区,

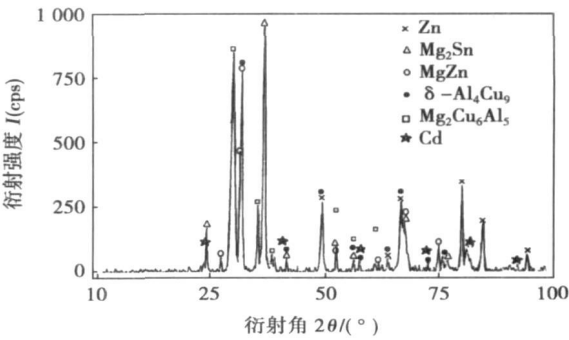


图 2 钎焊接头界面区的 XRD 图

Fig 2 X-ray diffraction gram of interfacial region in soldered joint

表 3 钎焊接头组织的微区成分分析

Table 3 Composition of microstructure of soldering joint

测试点	组织特征	成分(质量分数, %)			
		Zn	Cd	Al	Cu
1	白色基体	1.44	98.56	—	—
2	深灰色块状组织	97.28	1.10	0.82	0.80
3	黑色小颗粒组织	19.41	43.6	34.55	2.39
4	深灰色块状组织	84.97	—	0.40	14.63
5	浅色基体	1.32	98.68	—	—
6	靠近母材界面区点状组织	78.13	5.74	3.51	12.63

如果该区域有大量或连续分布的化合物产生, 整个钎焊接头的性能就会大大降低. 因此该区域是钎焊接头的薄弱区域^[3-5].

钎焊接头界面区的精细微观组织形貌和结构见图 3~图 5. 图 3 是镉及其氧化物、CdSn_{1.9}的形态及它们的电子衍射图. 镉是密排六方结构, CdSn_{1.9}为六方结构, CdO 为面心立方结构. 在 X 射线衍射分析时并未发现 CdSn_{1.9}及 CdO, 这是因为, 这类物相的含量很少, 其 X 射线的衍射强度低, 表现为衍射峰

很小或几乎没有, 难以发现和确定. 从图 3 可以看出, 细小的黑色 CdSn_{1.9}呈条状分布在镉的基体上, 对基体的性能产生不利的影响, 但由于 CdSn_{1.9}的数量少且细小, 因此对整个接头的性能影响很小. 另外界面区还有一些锡的氧化物及 η -Zn 的固溶体组织(图 4). SnO 为正交结构, SnO₂ 为简单立方结构, CdSnO₃ 是六方结构, 锡的氧化物主要以细小的颗粒分布在基体上, SnO 分布在镉的晶粒内部, 而 SnO₂ 主要分布在晶界上. 从图中还可以看出 SnO₂ 的颗

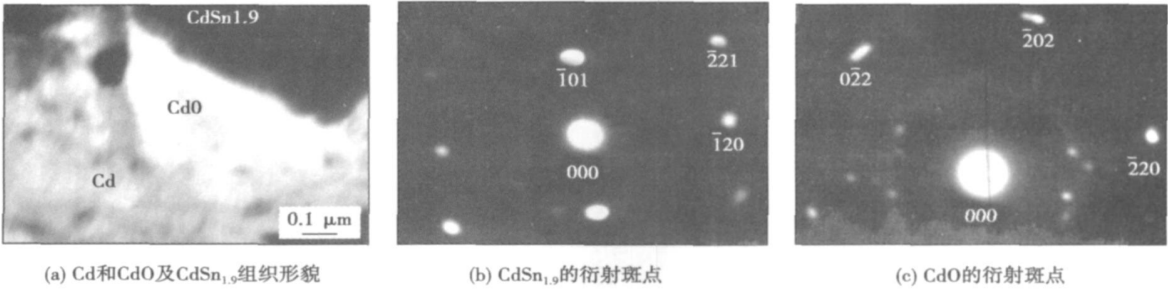


图 3 钎焊界面区 Cd 和 CdO 及 CdSn_{1.9}组织形貌及电子衍射图
Fig. 3 TEM image and electron diffraction spot of Cd, CdO and CdSn_{1.9} of soldering joint

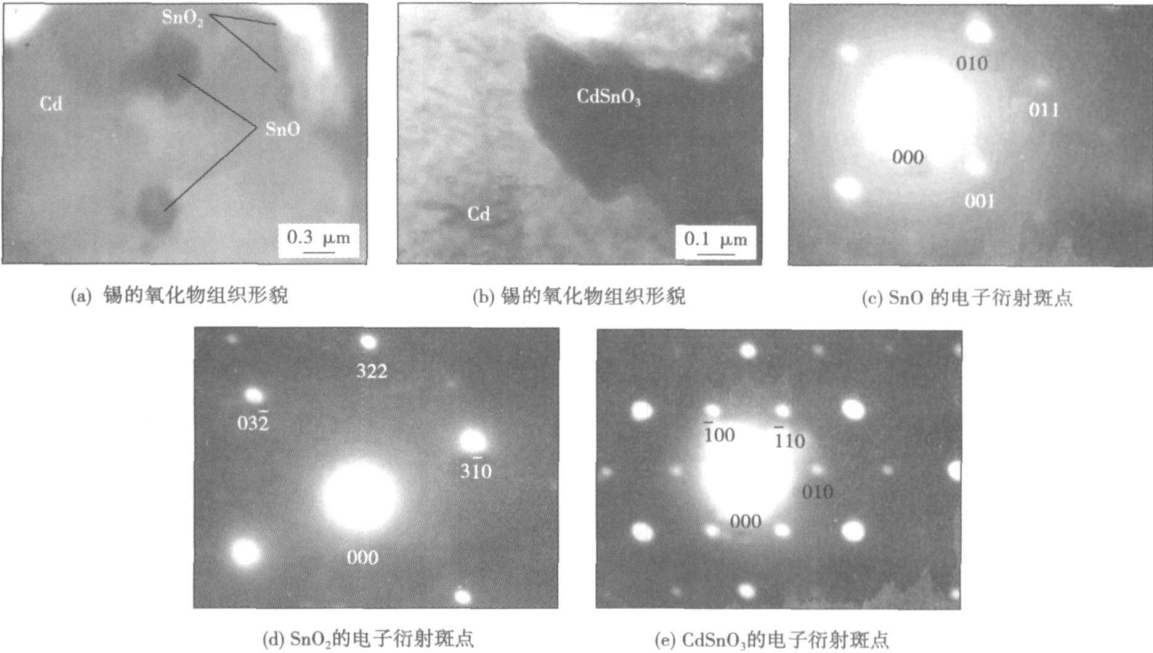


图 4 锡的氧化物 TEM 组织形貌及电子衍射图
Fig. 4 TEM image and electron diffraction spot of Sn oxide

粒比 SnO 的颗粒细小, 这些细小的氧化物颗粒, 不会对钎焊接头的性能产生不利的影响^[6].

钎焊接头界面区的组织中除了镉、 η -Zn 之外,

还有其它一些金属化合物(图 5). Mg₂Cu₆Al₅ 呈细小的块状分布在镉的基体上, 而黑色的 Al₄Cu₉ 细颗粒则分布在较大颗粒的 Mg₂Sn 上及其周围, 这些金属

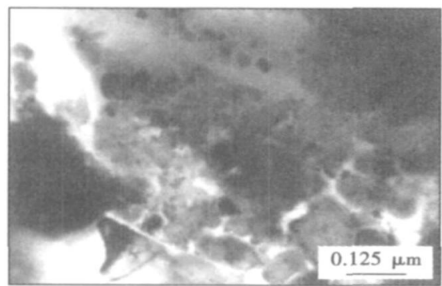


图 5 界面区的化合物 TEM 组织形貌
Fig. 5 TEM image of compounds in interface region

化合物以点状或颗粒状分布在基体上, 细小且不连续, 因此不会对基体产生不利的影响, 反而可以强化基体, 提高钎焊接头的性能^[7,8]。

3 结 论

- (1) 钎焊接头界面区主要有扩散区和溶解区组成, 靠近钎缝的扩散区含有较多的镉基固溶体 (1.44%Zn), 靠近母材的溶解区含有较多的锌基固溶体。
- (2) 界面区的相组成较复杂, 主要由镉、锡、锌、铝固溶体及一些氧化物 SnO, SnO₂, CdO 和金属化合物 MgZn, Mg₂Sn, Al₄Cu₉, Mg₂Cu₆Al₅ 等。
- (3) 界面区未发现对钎焊接头性能影响不利的连续状金属化合物层。少量的点状和颗粒状金属化合物有利于强化基体, 提高接头的强度。

参考文献:

[1] Prasad B K, Pattwardhan A K, Yegneswaran A H. Zinc-based alloy and comparison with bearing alloy [J] . Material Engineering Performance, 1998, 7(1): 1—3.

[2] Prasad B K. Tensile properties of some zinc-based alloys comprising 27.5% Al effects of alloy microstructure composition and test conditions [J] . Material Science and Engineering 1998 245 A: 257—266.

[3] Liu Xiuzhong, Dong Boling, Zhao Dongjian, *et al.* Microstructures and properties of tungsten inert gas welding joint of super-eutectic ZA alloy [J] . Transactions of Nonferrous Metals Society of China, 2001, 11(3): 387—390.

[4] Liu Xiuzhong, Yang Min, Xing Zhaohui, *et al.* Composition and microstructure characteristics in bond area of TIG welding for high strength ZA alloy [J] . Transactions of Nonferrous Metals Society of China, 2003, 13 (1): 153—157.

[5] 刘秀忠, 邹增大, 杨德新, 等. Zn-Al-Cu-Mg 合金气焊接头显微组织的分析研究 [J] . 材料导报, 2004, 18(10): 364—366.
Liu Xiuzhong, Zou Zengda, Yang Dexin, *et al.* Analysis and investigation of microstructure of oxy-acetylene welding joint of Zn-Al-Cu-Mg Alloy [J] . Material Review, 2004, 18(10): 364—366.

[6] Zhang Yongzhen, Chen Darou, Wei Shizhong, *et al.* Friction and wear behavior of welded zone of zinc-based alloy [J] . Moxaxue Xuebao/Tribology, 2000, 20(5): 340—343.

[7] Liu Liming, Tan Jinhong, Liu Xujing. Reactive brazing of Al alloy to Mg alloy using zinc-based brazing alloy [J] . Materials Letters, 2007, 61(11—12): 2373—2377.

[8] Prasad B K. Tensile properties of some zinc-based alloys comprising 27.5% Al Effects of alloy microstructure, composition and test conditions [J] . Microstructure and Processing, 1998, 245(2): 257—266.

作者简介: 刘秀忠, 女, 1962 年出生, 博士, 教授. 主要研究方向为钎焊、焊接质量检测及控制. 发表论文 50 余篇.
Email: liuxz@sdu.edu.cn

Materials Science and Engineering, Shenyang University of Technology, Shenyang 110178, China). p 73—76

Abstract The nickel-base alloy was deposited on the low carbon steel by plasma arc surfacing with transverse magnetic field. The influence of transverse alternative pulsed magnetic field frequency on microstructure and properties of plasma arc surfacing layer was researched. The hardness, wear resistance and microstructure of surfacing layer at different pulsed magnetic field currents were systematically analyzed by optical electronic microscope, wear test and microscopic hardness test. The results indicated that the transverse alternative pulsed magnetic field can effectively improve the crystal shape in plasma arc surfacing layer and refine crystal grain. With the proper pulsed magnetic field frequency, the optimum effect of electromagnetic stirring can be obtained, the amount of hardening phase in overlay deposit is increased, the growth direction of hardening phase can be controlled and the hardness and wear resistance of the surfacing overlay are improved.

Key words: plasma arc; transverse magnetic field; microstructure; wear resistance

3D reconstruction technology of SMT solder joint by shape from shading based on improved illumination model ZHAO Huihuang¹, ZHOU Dejian^{2,3}, HUANG Chunyue³ (1. School of Mechanical and Electrical Engineering, Xidian University, Xi'an 710071, China; 2. Department of Mechanical Engineering, Guangxi University of Technology, Liuzhou 545006, Guangxi, China; 3. School of Mechanical and Electrical Engineering, Guilin University of Electronic Technology, Guilin 541004, Guangxi, China). p 77—80

Abstract: Three-dimensional shape and its accuracy are dissatisfactory because of the highlight caused by specular reflection when the shape from shading is used to reconstruct the three-dimensional soldered joint. An improved illumination model is proposed, which can modify the diffuse reflectance component based on the features of image shooting, make a linear superposition for both specular reflection component and diffuse reflectance component. Then the improved illumination model is used to reconstruct the three-dimensional soldered joint after dealing with the soldered joint image by the proper image processing arithmetic. The experimental results show that the 3D shape by SFS based on the improved illumination model is more satisfactory in decreasing specular reflection influence than that of the traditional methods.

Key words: surface mount technology; three-dimensional reconstruction; shape from shading; illumination model; image processing

Reliability analysis of PBGA soldered joints based on Taguchi method DAI Wei, XUE Songbai, ZHANG Liang, JI Feng (College of Materials Science and Technology, Nanjing University of Aeronautics and Astronautics, Nanjing 210016, China). p 81—84

Abstract: In order to evaluate the reliability of PBGA soldered joints, an optimized method was proposed based on Taguchi design and numerical simulation, in which the Anand equation was used to describe the viscoplastic behavior of Sn3.0Ag0.5Cu solder, and the distribution of equivalent stress and strain in soldered joints under temperature cycle were studied respectively. Results indicate that the thermal fatigue life of soldered joints can be substantially improved by filling up the underfill between the PCB and substrate.

The linear expansion coefficients of substrate, epoxy mold compound, underfill and PCB were considered as the controlling factors, and the linear expansion coefficient of the substrate and that of epoxy mold compound were deemed to be the main influencing factors by Taguchi method. The optimized controlling factor combination can be decided as A3B3C3D3, and the verification test shows the maximum equivalent strain of the optimization scheme was decreased by 41.4%, and the ratio of signal to noise was increased by 4.61 dB.

Key words: plastic ball grid array; underfill; Taguchi method; linear expansion coefficient

Contact reactive brazing between Al alloy/Cu/stainless steel and analysis on grain boundary penetration behaviors WU Mingfang^{1,2}, SI Naichao¹, PU Juan² (1. Jiangsu University, Zhenjiang 212013, Jiangsu, China; 2. Jiangsu University of Science and Technology, Zhenjiang 212003, Jiangsu, China). p 85—88

Abstract Grain boundary penetration behavior occurs easily in the Al/Cu contact reactive brazing. In this paper, the mechanisms of formation and evolution of grain boundary penetration were investigated when contact reactive brazing between 6063 Al Alloy and 1Cr18Ni9Ti stainless steel was conducted using Cu as interlayer. The results show that the grain boundary penetration phenomenon is prominent. Grain boundary penetration depth was up to 200 μm when the brazing temperature was 570 $^{\circ}\text{C}$ and holding time was 60 min. The diffusion of atom into grain boundary was not sufficient but necessary for forming of grain boundary penetration. The key factor to induce grain boundary penetration was non-equilibrium diffusion of atom between the grain boundary and base metal, which led to crystal lattice expanding, and promoted the vacancy transferring into grain boundary, and resulted in a thin groove. And then, microcracks were formed in the grain boundaries, the eutectic liquid was sucked into the groove by capillary force, and finally grain boundary penetration was created. The interface reactive layer consisted of Fe-Al intermetallics (IMCs) in the side of 1Cr18Ni9Ti, the adjacent zone was Cu-Al IMCs, welded seam zone was composed of Al-Cu eutectic structure and large blocked Al solid solution.

Key words: Al Alloy; stainless steel; contact reactive brazing; grain boundary penetration; structure

Reaction mechanism and microstructure of interface in soldered joint of zinc based alloy LIU Xiuzhong^{1,2}, YANG Min^{1,2}, LIU Xinghong³ (1. Key Laboratory of Liquid Structure and Heredity of Materials (Ministry of Education), Shandong University, Jinan 250061, China; 2. School of Materials Science and Engineering, Shandong University, Jinan 250061, China; 3. Xiangshan Tongjia Foundry-die Plant, Xiangshan 315700, Zhejiang, China). p 89—92

Abstract The micro-region compositions, fine microstructure and phases of interface region in joint soldered with new solder and flux self-developed were studied by means of XRD, EPMA, TEM and SEM. The results show that the interface region mainly consists of diffusion zone and dissolution zone. There was more Cd based solid solution (1.44% Zn) in diffusion zone, while more Zn based solid solution in dissolution zone. The interface region mainly consists of Cd, Sn, Zn, Al solid solution, and oxides such as SnO, SnO₂, CdO and metallic compounds such as MgZn, Mg₂Sn, Al₄Cu₉ and Mg₂Cu₆Al₅. No continuous intermetallic compounds layer which

would seriously impair the properties of the soldered joint is found.

Key words: Zn based alloy; interfacial zone; reaction mechanism; microstructure

Finite element analysis on reliability of lead-free soldered joints for CSP device

YE Huan, XUE Songbai, ZHANG Liang, WANG Hui (College of Materials Science and Technology, Nanjing University of Aeronautics and Astronautics, Nanjing 210016, China). p 93—96

Abstract: Finite element method was employed to analyze the reliability of soldered joint in a CSP device. Anand model was used to establish the constitutive equation of Sn3.0Ag0.5Cu solder; the stress behavior of soldered joint was studied. The results indicate that the maximal stress is located at the upper surface of the soldered joint which is under the outermost of chip. The phenomenon of stress relaxation and accumulated enhancement could be observed obviously from the curves of stress and temperature with time cycle. Reliability of soldered joints with three usually-used heights are compared, and the results shows that the 0.35 mm×0.18 mm one has the best reliability. Moreover, the influence of chip thickness on the reliability of soldered joints are investigated in the last part, the simulation result indicates that the influence is little.

Key words: chip scale package; lead-free soldered joint; reliability; finite element analysis

Numerical simulation on deposition process of duplex thermal barrier coating by plasma spraying

HOU Pingjun, WANG Hangong, WANG Liuying, YUAN Xiaojing (501 staff, The Second Artillery Engineering College, Xi'an 710025, China). p 97—100, 104

Abstract: Numerical simulation was performed by finite element analysis (FEA) to investigate the temperature and stress in a typical duplex thermal barrier coating. During the spraying process, the temperature of the back surface of substrate increases step by step, both the temperature and the stress of the coating fluctuate periodically within a wide range. After the deposition, the specimen was cooled to the room temperature slowly. The stresses become constant values, and the maximum radial tensile stress exists at the interface between the ceramic layer and the bonding layer, and the maximum axial and shear stresses exist at the interface, where is the concentrated stress area. The stresses of the middle interfaces are uniform. The maximum tensile stress on the ceramic layer surface is 423.7 MPa.

Key words: numerical simulation; plasma spraying; thermal barrier coatings; temperature field; residual stress

A disparity map segmentation algorithm for 3D reconstruction of weld workpiece

WANG Jun¹, LIANG Zhimin^{1,2}, GAO Hongning² (1. School of Materials Science and Technology, Hebei University of Science and Technology, Shijiazhuang 050018, China; 2. State Key Laboratory of Advanced Welding Production Technology, Harbin Institute of Technology, Harbin 150001, China). p 101—104

Abstract: In remote welding, the segmentation of disparity map is an important step to create 3D model of weld workpiece by stereo vision sensor. In this paper, the USF plane range image segmentation algorithm was introduced into disparity map segmentation,

and by a region combination step, the revised algorithm can deal with the disparity map containing cylinder surface. The combination step could be divided into boundary detecting and curve region relabeling. During boundary detection, the pixel at the boundary of the segmented region after plane segmentation was recorded. In curve region relabeling, the adjacent regions in the same curved surface were assigned with the same label by comparing the boundary pixels' normal direction and distance between them. A segmented result of disparity map of saddle workpiece is shown to prove the feasibility of the algorithm.

Key words: disparity map segmentation; stereo vision; 3D reconstruction; remote welding.

Integrated life prediction method of ball grid array soldered joint

CHEN Ying, KANG Rui (Department of System Engineering of Engineering Technology, Beijing University of Aeronautics & Astronautics, Beijing 100191, China). p 105—108

Abstract: To quickly estimate the soldered joint lifetime of the ball grid array package, the analytical model of the simplified stress distribution was founded and the thermal fatigue lifetime was calculated by the creep lifetime prediction model. When the precise results were needed, the three dimensional finite element model was founded and the stress distribution in soldered joint was calculated by Anand constructive function of ANSYS, then the thermal fatigue lifetime was given by the Darveaux model. The analytical method and the finite element method were integrated to a main program by the secondary development function of ANSYS. With this program, the lifetime of the soldered joint can be quickly estimated or precisely predicted with the packaging and soldered joint dimension, material parameters and the thermal cycle parameters. Results of the case show that the analytical model results are more sensitive to the variation of the parameters, while the analyzed results by finite element model are stable.

Key words: ball grid array package; soldered joint; analytical method; FEA; lifetime prediction

Effect of Ti content on microstructure toughness of deposited metal with flux cored wire

WANG Zheng¹, GUI Chibin¹, WANG Yuhua² (1. College of Naval Architecture & Power, Naval University of Engineering, Wuhan 430033, China; 2. Naval Military Delegation Room of 407 Factory, Luoyang 471039, Henan, China). p 109—112

Abstract: The effects of Ti content on microstructure characteristic of deposited metal with flux cored wire were investigated with different contents of Ti-Fe powder under the protection of CO₂ and Ar+20%CO₂. The results show that the inclusions in deposited metal are mainly complex oxides composed of MnO-TiO_x-Al₂O₃-SiO₂ in Si-Mn-Ti deoxidized flux cored wire. With the increasing of Ti content in flux cored wire, the content of Ti in the inclusions increases, and most of inclusions are in the range of 0.3~2.0 μm in diameter, which promote the formation of acicular ferrite, thus those contribute to the increased toughness of deposited metal. Dissociative Ti can improve the intensity and the rigidity of microstructure, but it does worse to the microstructure toughness when too much dissociative Ti gets into the microstructure of deposited metal.

Key words: Ti; deposited metal; inclusion; toughness